

Please cite the Published Version

Mudhaffer, Shaymaa, Althagafi, Rana, Haider, Julfikar , Satterthwaite, Julian and Silikas, Nick (2024) Effects of printing orientation and artificial ageing on martens hardness and indentation modulus of 3D printed restorative resin materials. *Dental Materials*, 40 (7). pp. 1003-1014. ISSN 0109-5641

DOI: <https://doi.org/10.1016/j.dental.2024.05.005>

Publisher: Elsevier

Version: Published Version

Downloaded from: <https://e-space.mmu.ac.uk/634622/>

Usage rights:  [Creative Commons: Attribution 4.0](https://creativecommons.org/licenses/by/4.0/)

Additional Information: This is an open access article which first appeared in *Dental Materials*, published by Elsevier

Enquiries:

If you have questions about this document, contact openresearch@mmu.ac.uk. Please include the URL of the record in e-space. If you believe that your, or a third party's rights have been compromised through this document please see our Take Down policy (available from <https://www.mmu.ac.uk/library/using-the-library/policies-and-guidelines>)



Effects of printing orientation and artificial ageing on martens hardness and indentation modulus of 3D printed restorative resin materials

Shaymaa Mudhaffer^{a,b,*}, Rana Althagafi^b, Julfikar Haider^{a,c}, Julian Satterthwaite^a, Nick Silikas^{a,**}

^a Division of Dentistry, School of Medical Sciences, University of Manchester, Manchester, UK

^b Substitutive Dental Sciences, Faculty of Dentistry, Taibah University, Madinah, Saudi Arabia

^c Department of Engineering, Manchester Metropolitan University, Manchester, UK

ARTICLE INFO

Keywords:

Resin composite
Dental restorative material
3D printing
Martens hardness
Indentation modulus
Artificial ageing, Temporary resin, Definitive resin

ABSTRACT

Background: Three-dimensional (3D) printing is increasingly used to fabricate dental restorations due to its enhanced precision, consistency and time and cost-saving advantages. The properties of 3D-printed resin materials can be influenced by the chosen printing orientation which can impact the mechanical characteristics of the final products.

Purpose: The objective of this study was to evaluate the influence of printing orientation and artificial ageing on the Martens hardness (HM) and indentation modulus (E_{IT}) of 3D-printed definitive and temporary dental restorative resins.

Methods: Disk specimens (20 mm diameter \times 2 mm height) were additively manufactured in three printing orientations (0°, 45°, 90°) using five 3D-printable resins: VarseoSmile Crownplus (VCP), Crowntec (CT), Nextdent C&B MFH (ND), Dima C&B temp (DT), and GC temp print (GC). The specimens were printed using a DLP 3D-printer (ASIGA MAX UV), while LavaTM Ultimate (LU) and Telio CAD (TC) served as milled control materials. Martens hardness (HM) and indentation modulus (E_{IT}) were tested both before and after storage in distilled water and artificial saliva for 1, 30, and 90 days at 37 °C.

Results: 90° printed specimens exhibited higher HM than the other orientations at certain time points, but no significant differences were observed in HM and E_{IT} between orientations for all 3D-printed materials after 90 days of ageing in both aging media. LU milled control material exhibited the highest HM and E_{IT} among the tested materials, while TC, the other milled control, showed similar values to the 3D printed resins. CT and VCP (definitive resins) and ND displayed higher Martens parameters compared to DT and GC (temporary resins). The hardness of the 3D-printed materials was significantly impacted by artificial ageing compared to the controls, with ND having the least hardness reduction percentage amongst all 3D-printed materials. The hardness reduction percentage in distilled water and artificial saliva was similar for all materials except for TC, where higher reduction was noted in artificial saliva.

Significance: The used 3D printed resins cannot yet be considered viable alternatives to milled materials intended for definitive restorations but are preferable for use as temporary restorations.

1. Introduction

In recent years, the landscape of dentistry has undergone a significant transformation due to the increasing prevalence of computer-aided design and manufacturing (CAD/CAM) technologies, and more recently, additive manufacturing (AM) or 3D-printing. Unlike traditional methods

or subtractive manufacturing, this technology reduces human errors, instrument wear, and material wastage without extending production time [1,2]. Within the dental field, stereolithography (SLA) and digital light processing (DLP) have emerged as the most frequently used AM technologies [3]. Both systems involve the gradual deposition of successive layers of photosensitive material, which swiftly polymerize to

* Corresponding author at: Division of Dentistry, School of Medical Sciences, University of Manchester, Manchester, UK.

** Corresponding author

E-mail addresses: Smudhaffer@Taibahu.edu.sa (S. Mudhaffer), Nikolaos.silikas@manchester.ac.uk (N. Silikas).

¹ Division of Dentistry, School of Medical Sciences, University of Manchester, Coupland Building 3, Oxford Road, Manchester, M13 9PL, UK.

<https://doi.org/10.1016/j.dental.2024.05.005>

Received 22 March 2024; Received in revised form 29 April 2024; Accepted 3 May 2024

Available online 11 May 2024

0109-5641/© 2024 The Author(s). Published by Elsevier Inc. on behalf of The Academy of Dental Materials. This is an open access article under the CC BY license (<http://creativecommons.org/licenses/by/4.0/>).

construct objects, offering unparalleled flexibility in shaping various dental prosthetic devices [4].

Critical processing parameters in 3D-printing such as printing orientation [5–8], build position [9], layer thickness [2,10,11], and support structure [12] significantly influence the final properties of the objects printed. Therefore, precise configuration of these parameters is vital to achieve high quality dental devices [13]. Notably, printing orientation has become a pivotal consideration given the anisotropic nature of the fabricated product due to the layered fabrication technique. Although anisotropy is generally viewed as a drawback, in dentistry it can be utilized advantageously by aligning the printing direction of the restoration with the specific load directions in the oral cavity. [8]. Previous studies have emphasized the significance of printing orientation in determining the properties of 3D-printed objects [5,7,9,14]. Moreover, researchers have explored Martens parameters in 3D-printed materials designed for temporary restorations [10,15–17] occlusal splints [18–20] and denture bases [21–23]. Martens hardness measurement is an established method for assessing the elastic-plastic properties of polymer-based materials and for detecting surface degradation, such as the one caused by extended exposure to an aqueous solution that mimics the clinical degradation within the oral cavity. Additionally, hardness values can be associated with the degree of conversion and the amount of filler in polymeric materials. However, when it comes to understanding the deformation behaviour of materials, the indentation modulus provides a more suitable metric, which can be linked to their clinical performance as well [16].

However, despite the introduction of composite resins for definitive restorative applications, there is a notable gap in the literature. To the best of the authors' knowledge, no studies have investigated the impact of printing orientation on the Martens hardness of these materials. Furthermore, the literature is lacking in reporting the effect of long-term artificial ageing in both distilled water (DW) and artificial saliva (AS) on the hardness of 3D printed resins. Therefore, the aim of this work was to investigate the impact of printing orientation on the Martens hardness (HM) and elastic modulus (E_{IT}) of 3D-printed dental restorative resins and compare with well-established resins used in subtractive manufacturing. The following null hypotheses were tested:

1. No significant difference exists, in relation to HM and E_{IT} , between the printing orientations (0° , 45° , and 90°) of 3D-printed resin composite materials after ageing at 1 day, 30 days and 90 days in DW and AS.
2. No significant difference exists, in relation to HM and E_{IT} , between the different commercially available 3D-printed and milled materials indicated for temporary and definitive restorations after ageing for 90 days in DW and AS.
3. No significant effect of storage duration (1d, 30d, 90d) on HM and E_{IT} of the investigated resin composite materials exists.
4. No significant difference exists, in relation to the hardness reduction percentage, between the two-ageing media (DW and AS)

2. Materials and methods

2.1. Materials and study design

Seven commercially available resin-composite materials were utilized in this study for additive manufacturing (3D printing) and subtractive manufacturing (milled). The materials investigated, along with their respective chemical compositions as per the manufacturers' data, are summarized in Table 1. Baseline measurements were recorded under dry conditions 24 h after preparation ($\pm 23^\circ\text{C}$). Measurements were subsequently recorded after 1, 30, and 90 days of storage in distilled water (DW) and artificial saliva (AS) at 37°C . Fig. 1 graphically illustrates the study design and represents number of specimens in each group and sub-group.

2.2. Specimen preparation

2.2.1. Additive manufacturing group

Disk specimens were fabricated in three different orientations (0° , 45° , 90°) with dimensions of 20 mm (diameter) \times 2.3 mm (height). These three orientations were chosen to cover a range of possible angles for printing FDP's: horizontal, vertical, and angular directions. Specimens were designed using a free online software Tinkercad, saved as STL files, and then imported into a CAM software, Composer (version 1.3.2, 2021, ASIGA, Australia). Printing parameters, including orientation (0° , 45° , and 90°), number of specimens ($n = 12$ per orientation), layer thickness ($50\ \mu\text{m}$) and support design and quantity (automatically configured), were chosen before initiating the printing process (Fig. 2A). To prevent cross-contamination, each material had its own dedicated resin tray. The specimens were 3D printed using the ASIGA MAX UV 3D printer (ASIGA, Australia), which is an open system printer utilizing DLP technology with a light wavelength of 385 nm.

Each material group was subdivided into three subgroups based on the printing orientation of the specimens. The 0° specimens were printed horizontally, with layers stacked along the width of the specimen which was placed flat on the building platform. The 45° specimens were printed at a 45° angle to the build platform. Lastly, the 90° specimens were printed vertically, with layers stacked sequentially along the height of the specimen. The direction of the force on the specimen surface during flexural strength test with respect to the layer orientation is presented in (Fig. 2B). In total, 180 3D-printed specimens were prepared.

After printing was completed, the specimens underwent a 5-minute cleaning process in ethanol using Form Wash (Formlabs Inc., USA) to remove any residual surface monomer. They were then patted dry with a paper towel. Next, the support structures were removed from the specimens using a scalpel, and the specimens were placed in a light-curing box according to the manufacturer's recommendations for each material. The specifications for light curing units and post fabrication parameters for different materials with corresponding times or number of flashes are listed in Table 2.

In accordance with the guidelines established by the International Organization for Standardization for HM measurements (ISO 14577–4, 2016), all specimens underwent mechanical polishing using a Metaserve 250 grinder-polisher (Buehler, Lake Bluff, Illinois). This polishing process aimed to achieve a smooth, parallel, and consistent surface by employing a series of successive silica carbide (SiC) papers, ranging from P600 to P4000 grit (Buehler Co, Illinois, USA), while ensuring continuous water cooling for 20 s on each side. Subsequently, the specimens were polished using $0.25\ \mu\text{m}$ MetaDi™ Supreme diamond suspension and a $0.05\ \mu\text{m}$ MasterPrep alumina suspension (Buehler Co, Illinois, USA).

Finally, all specimens were subjected to five-minute ultrasonic cleaning in deionized water (DW) using an Ultrasonic Cleaning System (L & R Co, NJ, USA). The final specimen dimensions were $20 \times 2\ \text{mm}$, verified with an electronic digital calliper (PDC150M, Draper Tools Ltd, Hampshire, UK) (ISO 10477, 2020, and ISO 4049), ensuring an accuracy of $\pm 0.1\ \text{mm}$. They were then stored in dry and dark conditions for a 24-hour period to allow complete polymerization before conducting HM and E_{IT} measurements.

2.2.2. Control groups

Specimens from subtractive CAD/CAM blocks, specifically Lava Ultimate and Telio CAD, were cut into sections ($14 \times 14 \times 2\ \text{mm}$) using a diamond blade (MK 303; MK Diamond, CA, USA) mounted on a saw (Isomet 1000 Precision Saw; Buehler Co, IL, USA) with a continuous water supply ($n = 12$). Following this, the specimens were subjected to the same polishing and cleaning process as the additive manufacturing groups. To ensure precision, the dimensions of the specimens were verified using an electronic digital calliper (PDC150M, Draper Tools Ltd, Hampshire, UK) with an accuracy of $\pm 0.01\ \text{mm}$. This specific size was

Table 1
Manufacturers' compositional information of investigated resin materials.

	Material	Code	Manufacturer	Composition	wt%	Lot. #	Shade	Indications
3D printed	Varseosmile Crown ^{plus}	VCP	BEGO, Germany	Esterification products of 4,4'-isopropylidiphenol, ethoxylated and 2-methylprop-2enoic acid	5-75	600414	A2	Permanent crowns, inlays, onlays, and veneers
				Silanized dental glass	-			
				Diphenyl (2,4,6-trimethylbenzoyl) phosphine oxide	< 2.5			
	Crowntec	CT	Saremo Dental AG, Switzerland	Methyl benzoylformate	-			
				Total filler content (particle size 0.7 µm)	30-50			
				Bis-EMA	50-75			
				Trimethylbenzoyldiphenyl phosphine oxide	0.1 - < 1			
	NextDent C&B MFH	ND	3D systems, Netherlands	Silanized dental glass, pyrogenic silica, catalyst and Inhibitors	-			
				Total filler content (particle size 0.7 µm)	30-50			
				7,7,9(or 7,9,9)-trimethyl-4,13-dioxo-3,14-dioxo-5,12-diazahexadecane-1,16-diyl bismethacrylate	50-75			
2-hydroxyethyl methacrylate (HEMA)				< 25				
Ethoxylated bisphenol A dimethacrylate				< 10				
Ethylene dimethacrylate				< 10				
Silicon dioxide				1-5				
Diphenyl (2,4,6-trimethylbenzoyl) phosphine oxide				1-5				
Mequinol; 4-methoxyphenol; hydroquinone monomethyl ether				< 0.1				
Titanium dioxide				< 0.1				
Dima C&B temp	DT	Kulzer, Germany	Esterification products of 4,4'-isopropylidiphenol, ethoxylated and 2-methylprop-2enoic acid	40-60				
			7,7,9(or 7,9,9)-trimethyl-4,13-dioxo-3,14-dioxo-5,12-diazahexadecane-1,16-diyl bismethacrylate	30-50				
			Propylidynetrimethyl trimethacrylate	3-10				
			Diphenyl (2,4,6-trimethylbenzoyl) phosphine oxide	< 3				
			Mequinol	< 1				
			UDMA	50-75				
			2,2'-ethylenedioxydiethyl dimethacrylate	10- < 25				
			Esterification products of 4,4'-isopropylidenediphenol, ethoxylated and 2-methylprop-2-enoic acid	2.5- < 5				
			Quartz (silicon dioxide)	10- < 25				
			Diphenyl (2,4,6-trimethylbenzoyl) phosphine oxide	< 2.5				
GC temp print	GC	GC dental, Japan	2-(2 H-benzotriazol-2-yl)-p-cresol	0.1-< 0.2				
			BisGMA, UDMA, BisEMA, TEGDMA	20				
			Silica nanomers (20 nm)	80				
			Zirconia nanomers (4- 11 nm)					
			Silica-zirconia nanoclusters (0.6-10 µm)					
			Polymethyle methacrylate	99.5				
			Pigments	< 1				
Milled	Lava TM Ultimate	LU	3 M ESPE, USA			NC95259	A2	Permanent single unit restorations, inlays, onlays and veneers
	Telio CAD	TC	Ivoclar vivadent AG			Z02TYX	A2	Single- and multiple-unit temporary restorations

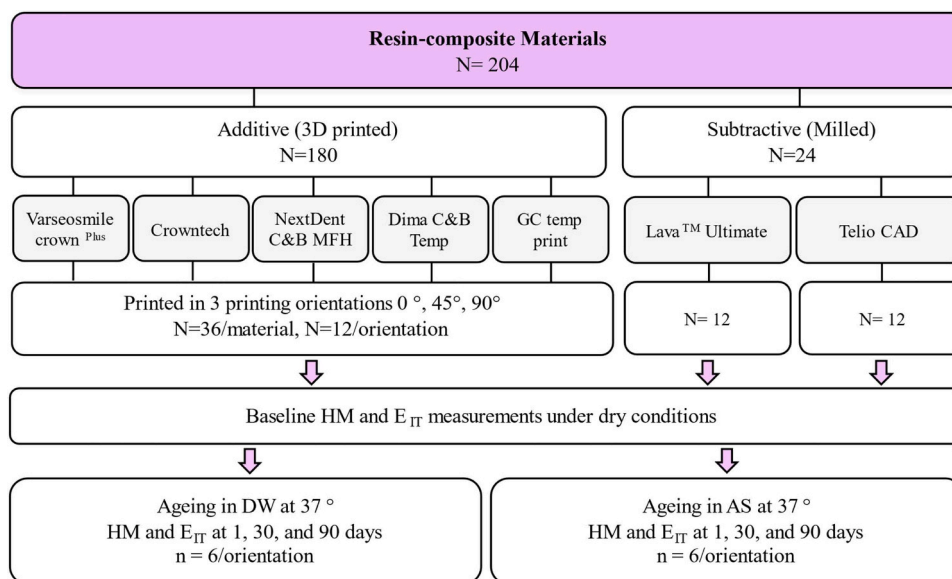


Fig. 1. Description of the study design.

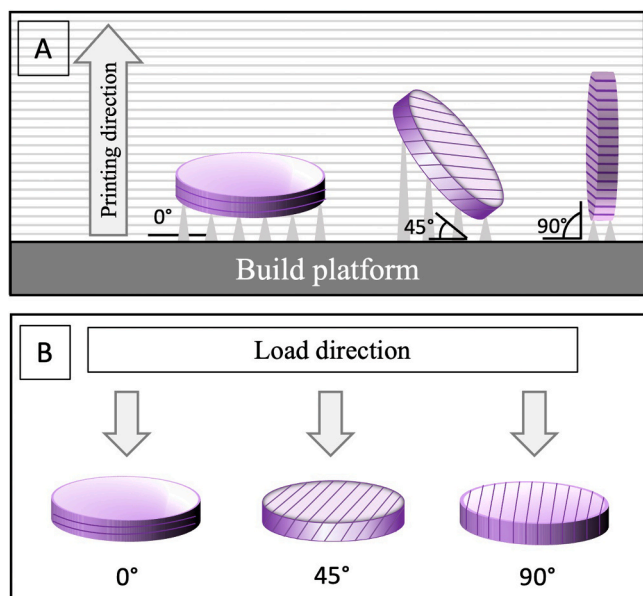


Fig. 2. A. Schematic representation of the print design of disc-shaped specimens in 0°, 45°, and 90° print orientations. B. Direction of the force on the specimen surface during flexural strength test with respect to the layer orientations.

chosen to accommodate the size restrictions of the milled blocks.

2.3. Artificial ageing

To simulate accelerated aging, the specimens were arranged within a light-protected container. Inside this container, a 3D-printed custom specimen holder, fabricated from model resin (ASIGA, Australia), was used to position the specimens in a vertical position, ensuring that both surfaces came into contact with their assigned storage solutions, either AS or DW. Subsequently, they were placed within a Heraeus incubator (BB 16-Function Line; Kendro, Hanau, Germany) held at a consistent temperature of 37 °C. To prevent saturation resulting from product degradation, the storage solutions were refreshed after every four weeks. Artificial Saliva was prepared using sodium chloride (0.4 g),

Table 2

Post curing device parameters and curing parameters used for the 3D-printed resin materials.

	Post curing device		
	Form cure	Otoflash G171	Cara print LED cure
Manufacturer	Formlabs, USA	NK-Optik, Germany	Kulzer, Germany
Technology	Ultraviolet light (UV)	Flashlight	Light-emitting diode (LED)
Number of light sources	13	2	10
Light intensity	39 Watt	200 Watt	15-150 Watt
Light spectrum (wavelength)	405 nm	280-700 nm (peak 400-500 nm)	370-470 nm (peak 397-450 nm)
Maximum temperature	60-80 °C	n/a	10-30 °C
Materials and Curing recommendation	Nextdent C&B MFH (60 °C for 30 min)	Varseosmile Crown ^{plus} (2 × 1500 flashes) Crowntec (2 × 2000 flashes) GC Temp Print (2 × 400 flashes)	Dima C&B Temp (60 °C for 20 min)

potassium chloride (0.4 g), calcium chloride (0.795 g), sodium dihydrogen phosphate (0.69 g) and sodium sulphide hydrate (0.005 g) mixed with 1000 ml distilled water [24,25]. The pH of AS was found to be 5.3 using a digital microprocessor pH meter (DELTA 340, Mettler Toledo).

2.4. Marten's hardness and indentation measurement

Measurements for HM and E_{IT} were initially conducted under dry conditions (baseline), and subsequently after 1, 30, and 90 days of aging in DW and AS. These measurements were carried out using a Zwick Martens Hardness Instrument (Z2.5, ZwickRoell Ltd) equipped with a Vickers hardness measurement tip (136°).

A rigid custom specimen holder shaped from putty was made to prevent any specimen displacement during the measurement process and to maintain consistent specimen placement at each measurement occasion. Once the specimen was secured in place, a force was applied

with a loading speed of 5 N/s, reaching up to 10 N, held for 30 s, and then released at a rate of 5 N/s. The initial approach rate was set at 100 mm/min, while the speed of the indenter tip until initial contact was 40 mm/min. The sensor tip distance from each specimen after the initial contact was 40 μm .

Four force-controlled indentations were performed on each specimen surface under dry conditions, and this process was repeated at each storage interval. To ensure that measurements were taken without overlap, a 3 mm spacing was kept between indentations. All data presented in this study represent the mean of these multiple indentations.

The test load and indentation depth were automatically recorded during the loading and unloading of the Vickers indentation tip, creating load-displacement curves. HM values, in addition to E_{IT} values, were automatically obtained using the TestXpert® software (Zwick GmbH and Co).

Following ISO 14577-4 (2016), Eqs. (1) and (2) were used for calculating HM and E_{IT} :

$$HM = \frac{F}{A_s(h)} = \frac{F}{26.43 \times h^2} \quad (1)$$

$$E_{IT} = (1 - \nu_s^2) \times \left(\frac{1}{E_\gamma} - \frac{(1 - \nu_i^2)}{E_i} \right) \quad (2)$$

HM was measured in N/mm^2 ; F (test force) in N, $A_s(h)$ is the surface area of the indenter at a distance h from the tip in mm^2 . E_{IT} was recorded in kN/mm^2 ; E_γ is the reduced modulus of the indentation contact, whereas E_i is the elastic modulus of the indenter [26]; ν_s and ν_i are the Poisson's ratios of the specimens and indenter respectively, with $\nu_s = 0.35$ [27] and $\nu_i = 0.3$.

Following a 90-day storage period, the percentage of hardness reduction (HR%) was calculated, a method previously employed by Alamouh et al. [28]:

$$HR\% = \frac{HM(d_0) - HM(d_{90})}{HM(d_0)} \times 100 \quad (3)$$

Where $HM(d_0)$ and $HM(d_{90})$ are the Martens hardness numbers at day 0 and day 90, respectively.

2.5. Filler content assessment

In line with ISO 1172 (1996), the inorganic filler content proportion was determined by eliminating the organic component from the studied materials through a heating process known as the Ash technique. Disk specimens (12 mm \times 2 mm) from each material were printed with the same method detailed in 2.2.1 in a 0° orientation ($n = 3$). Each specimen was positioned on a crucible, placed in an electric furnace (Programat EP 5000; Ivoclar Vivadent, Liechtenstein, Austria) and subjected to a temperature of 600 $^\circ\text{C}$ for 30 min. Subsequently, the crucible containing the specimen was allowed to cool within a desiccator and then weighed using an electronic analytical balance, ensuring precision to 0.01 mg (Ohaus Analytical Plus; Ohaus Corporation, USA). The percentage of inorganic filler weight was then calculated (Eq. (3)) using the same method as described by Alharbi et al. [29].

$$\text{Filler weight.}\% = \frac{(w_3 - w_1)}{(w_2 - w_1)} \times 100 \quad (4)$$

Where w_1 represents the initial mass of the dry crucible, w_2 represents the initial mass of dry crucible combined with the dried specimen, and w_3 is the final mass of the crucible combined with the burnt specimen residue.

2.6. Surface morphology

The surface morphology of the specimens after printing and polishing was studied using an optical microscope (Echo, Revolve, California,

USA) with a magnification of $\times 10$.

2.7. Statistical analysis

Data analysis was conducted using a statistical software package (SPSS Inc., Chicago, IL, USA). To assess variance normality and homogeneity, Shapiro-Wilk and Levene's tests were applied, respectively. A multiple-way repeated measures ANOVA was executed to explore the interactions among the material group, storage time, storage media, and print orientation concerning HM/ E_{IT} . Additionally, two-way repeated measures ANOVA, one-way repeated measures ANOVA, and Tukey's Post-Hoc test ($p \leq 0.05$) were employed to clarify the interactions both within and between these variables. T-test was performed to investigate the difference between the ageing media. Pearson correlation analysis was conducted to investigate the relationship between filler weight and HM and E_{IT} . All tests were conducted at a significance level of $\alpha = 0.05$. The sample size was calculated based on a pilot study using G*power software (V.3.1.3; Heinrich Hein University, Germany). This showed that repeated ANOVA has a power of 92% to detect differences in HM with sample size: $n = 12$ ($\alpha = 0.05$).

3. Results

3.1. Martens hardness and indentation modulus

Means and standard deviations for HM and E_{IT} of the studied materials are listed in Tables 3 and 4 and presented graphically in Fig. 3. The results indicated a significant main effect for material, printing orientation and ageing time on HM and E_{IT} ($p < 0.05$). The material (HM: $\eta_p^2 = 0.9$, E_{IT} : $\eta_p^2 = 0.8$, $p < 0.05$) and storage time (HM and E_{IT} : $\eta_p^2 = 0.9$, $p < 0.05$) had the most impact on HM and E_{IT} , followed by print orientation (HM and E_{IT} : $\eta_p^2 = 0.05$, $p < 0.05$). The difference in hardness reduction exerted by DW and AS was found to be not statistically significant ($p = 0.6$). A strong positive correlation between filler weight and HM ($r = 0.87$, $p < 0.001$) and filler weight and E_{IT} ($r = 0.85$, $p < 0.001$) was found.

3.1.1. Printing orientation

Initially, when evaluated under dry conditions, there were no statistically significant variations in HM and E_{IT} among different orientations for all the 3D printed materials, except for ND (where HM: $90^\circ > 0^\circ \geq 45^\circ$) and VCP (where HM: $0^\circ \geq 45^\circ > 90^\circ$), revealing slight but statistically significant differences ($p = 0.005$, $p = 0.003$, respectively). The hardness of the 3D printed materials under dry condition ranged from 121.23 to 197.98 N/mm^2 for specimens printed at 0° , 110.17 to 197.98 N/mm^2 for those printed at 45° , and 127.09 to 203.23 N/mm^2 for those printed at 90° . Subsequent to one day of wet storage, a noticeable trend emerged in specimens printed with a 90° orientation, as they exhibited slightly higher HM compared to the 45° printed specimens for all 3D printed materials. However, this difference was statistically significant only for VCP, DT (in DW) ($p = 0.02$, $p = 0.001$, respectively), and GC (in both aging media) ($p = 0.01$). Similar trends in HM continued at 30 days of aging for ND (in both aging media) and GC (in AS), where 90° printed specimens maintained statistically significantly higher HM than those printed at 0° and 45° orientations ($p < 0.001$), whereas no significant difference was observed between orientation for the remaining materials. Differences in E_{IT} between orientations varied depending on the specific 3D printed materials. However, at the end of the ageing period (90 days), no significant differences were observed in HM and E_{IT} between orientations for all 3D printed materials in both aging media.

Considering that the 90° specimens exhibited higher mechanical properties and to compare with similar studies [16,30], this printing orientation was selected as the reference point for all comparisons among the remaining independent parameters (materials, aging time, and aging media).

Table 3

Martens hardness means and standard deviations (N/mm²) of additively manufactured resin materials printed with three orientations (0°, 45°, and 90°) after ageing in distilled water and artificial saliva for 90 days at 37 °C (n = 6).

Category	Material	Orientation	Baseline (dry)	Distilled water			Artificial saliva		
				1d	30d	90d	1d	30d	90d
Definitive 3D printed	VCP	0	194.8 (3.9) ^a	185.4 (2.5) ^{ab}	205.4 (5.3) ^a	104.7 (2.7) ^a	186.0 (2.1) ^a	205.1 (2.7) ^a	103.1 (3.2) ^a
		45	194.3 (4.6) ^a	184.6 (3.6) ^a	203.2 (4.2) ^a	101.4 (3.2) ^a	184.2 (2.7) ^a	201.4 (2.1) ^a	98.8 (2.9) ^a
		90	187.1 (2.5) ^b	190.3 (4.1) ^b	200.1 (4.1) ^a	100.6 (2.8) ^a	188.5 (4.4) ^a	202.3 (3.3) ^a	102.9 (4.0) ^a
	CT	0	197.9 (4.9) ^a	204.2 (3.0) ^a	217.5 (3.8) ^a	102.1 (4.0) ^a	203.9 (3.4) ^a	217.6 (4.5) ^a	106.9 (3.1) ^a
		45	197.9 (3.8) ^a	202.1 (1.7) ^a	214.8 (2.1) ^a	100.2 (2.2) ^a	202.5 (1.8) ^a	213.3 (2.3) ^a	103.4 (5.6) ^a
		90	203.2 (5.5) ^b	203.2 (1.8) ^a	214.6 (5.7) ^a	104.1 (1.1) ^a	201.5 (1.2) ^b	214.7 (2.6) ^a	102.6 (4.5) ^a
Temporary 3D printed	ND	0	143.6 (5.1) ^a	113.3 (7.8) ^a	112.3 (3.3) ^a	101.4 (3.5) ^a	108.2 (5.4) ^a	110.7 (4.1) ^a	101.9 (4.3) ^a
		45	144.3 (5.9) ^a	115.8 (3.4) ^a	115.3 (2.4) ^a	104.9 (3.2) ^a	115.8 (5.3) ^a	115.2 (2.6) ^a	102.4 (3.7) ^a
		90	153.7 (3.8) ^b	120.8 (5.0) ^a	123.1 (3.0) ^b	102.9 (2.7) ^a	117.4 (7.9) ^b	124.2 (2.6) ^b	101.2 (4.8) ^a
	DT	0	133.5 (8.5) ^a	121.2 (7.0) ^a	99.7 (5.8) ^a	64.6 (2.7) ^a	111.0 (6.9) ^a	98.5 (1.9) ^a	60.8 (5.8) ^a
		45	126.6 (12.3) ^a	110.8 (3.6) ^b	99.7 (4.3) ^a	66.5 (5.1) ^a	108.1 (6.4) ^a	101.1 (2.2) ^a	64.4 (3.3) ^a
		90	127.4 (7.2) ^b	122.3 (3.6) ^a	102.7 (4.2) ^a	67.0 (4.4) ^{a,B,4}	111.9 (2.9) ^a	100.4 (4.0) ^a	66.7 (3.0) ^{a,B,4}
GC	0	121.2 (8.7) ^a	112.0 (9.5) ^{ab}	72.2 (4.1) ^a	66.9 (5.4) ^a	118.4 (13.3) ^a	70.5 (4.0) ^a	66.6 (5.4) ^a	
	45	110.2 (16.2) ^a	98.7 (18.2) ^a	73.2 (5.1) ^a	68.2 (3.5) ^a	98.1 (11.7) ^b	66.2 (4.9) ^a	65.3 (6.5) ^a	
	90	127.1 (8.3) ^b	123.1 (4.6) ^b	78.5 (4.3) ^{a,E,2}	72.9 (4.4) ^{a,B,2}	117.3 (7.7) ^b	79.3 (4.3) ^{b,D,2}	72.5 (2.9) ^{a,B,2}	
Milled	LU		606.4 (6.5) ^{E,1}	608.5 (17.1) ^{C,1}	644.3 (18.0) ^{F,2}	584.4 (14.8) ^{C,2}	602.5 (12.4) ^{D,1}	642.8 (19.4) ^{E,2}	579.7 (9.4) ^{C,3}
	TC		146.1 (7.1) ^{C,1}	135.4 (10.8) ^{B,1}	134.9 (2.8) ^{C,1}	119.0 (13.3) ^{D,2}	136.9 (5.7) ^{E,1}	134.3 (1.3) ^{B,1}	104.6 (12.0) ^{A,2}

a,b,c,d,e Describe significant differences between orientations within one 3D printed material and ageing time ($p < 0.05$). A,B,C,D,E Describe significant differences between materials within one ageing time ($p < 0.05$). 1,2,3,4 Describe significant differences between ageing times (compared to baseline) within one ageing media and one material ($p < 0.05$)

Table 4

Indentation modulus means and standard deviations (kN/mm²) of additively manufactured resin materials printed with three orientations (0°, 45°, and 90°) after ageing in distilled water and artificial saliva for 90 days at 37 °C (n = 6).

Category	Material	Orientation	Baseline (dry)	Distilled water			Artificial saliva		
				1d	30d	90d	1d	30d	90d
Definitive 3D printed	VCP	0	5.1 (0.2) ^a	5.1 (0.1) ^a	5.2 (0.1) ^a	1.9 (0.1) ^a	4.9 (0.1) ^a	5.2 (0.1) ^a	2.0 (0.1) ^a
		45	4.97 (0.1) ^a	4.8 (0.3) ^a	5.2 (0.2) ^{ab}	1.9 (0.1) ^a	4.9 (0.2) ^a	5.0 (0.1) ^a	1.9 (0.1) ^a
		90	4.9 (0.1) ^{a,AB,1}	5.1 (0.2) ^{a,A,1}	4.9 (0.2) ^{b,A,1}	1.8 (0.1) ^{a,ABC,2}	4.9 (0.1) ^{a,A,1}	5.0 (0.2) ^{a,A,1}	1.9 (0.1) ^{a,A,2}
	CT	0	5.6 (0.5) ^a	5.5 (0.1) ^a	5.6 (0.1) ^a	1.8 (0.1) ^a	5.5 (0.1) ^a	5.6 (0.1) ^a	1.9 (0.1) ^a
		45	5.2 (0.2) ^a	5.4 (0.1) ^a	5.4 (0.2) ^{ab}	1.8 (0.1) ^a	5.4 (0.1) ^a	5.3 (0.2) ^{ab}	1.9 (0.1) ^a
		90	5.3 (0.2) ^{a,A,1}	5.3 (0.1) ^{a,A,1}	5.3 (0.2) ^{b,A,1}	1.9 (0.1) ^{a,AB,2}	5.4 (0.2) ^{a,A,1}	5.2 (0.2) ^{a,A,1}	1.9 (0.1) ^{a,A,2}
Temporary 3D printed	ND	0	4.2 (0.3) ^a	3.4 (0.6) ^a	3.1 (0.4) ^a	2.1 (0.5) ^a	3.8 (0.3) ^a	3.3 (0.2) ^a	2.1 (0.6) ^a
		45	4.1 (0.2) ^a	3.3 (0.4) ^a	3.3 (0.2) ^{ab}	2.1 (0.2) ^a	3.6 (0.4) ^a	3.4 (0.1) ^a	1.9 (0.1) ^a
		90	4.4 (0.1) ^{a,BC,1}	3.6 (0.2) ^{a,B,2}	3.5 (0.1) ^{b,B,2}	2.3 (0.3) ^{a,A,3}	3.9 (0.2) ^{a,B,2}	3.7 (0.1) ^{b,B,2}	2.1 (0.2) ^{a,B,3}
	DT	0	3.0 (0.4) ^a	3.1 (0.3) ^a	1.8 (0.1) ^a	1.2 (0.1) ^a	2.1 (0.4) ^a	1.6 (0.1) ^a	1.1 (0.1) ^a
		45	3.0 (0.2) ^a	2.9 (0.2) ^a	2.0 (0.4) ^a	1.3 (0.1) ^a	2.1 (0.4) ^a	1.7 (0.1) ^a	1.1 (0.1) ^a
		90	2.9 (0.4) ^{a,D,1}	2.9 (0.2) ^{a,B,1}	1.8 (0.3) ^{a,C,2}	1.2 (0.1) ^{a,C,3}	2.2 (0.3) ^{a,D,2}	1.7 (0.1) ^{a,C,3}	1.2 (0.1) ^{a,B,4}
GC	0	3.2 (0.7) ^a	3.1 (0.5) ^{ab}	1.4 (0.1) ^a	1.3 (0.2) ^a	3.2 (0.5) ^a	1.4 (0.2) ^a	1.3 (0.1) ^a	
	45	2.9 (0.7) ^a	2.4 (0.9) ^a	1.5 (0.2) ^a	1.4 (0.1) ^a	2.4 (0.8) ^a	1.7 (0.9) ^a	1.3 (0.2) ^a	
	90	3.5 (0.4) ^{a,D,1}	3.4 (0.3) ^{b,C,1}	1.6 (0.1) ^{a,C,2}	1.5 (0.1) ^{a,BC,2}	2.8 (0.7) ^{a,CD,1}	1.7 (0.1) ^{a,C,2}	1.4 (0.1) ^{a,B,2}	
Milled	LU		12.6 (0.5) ^{E,1}	13.2 (0.7) ^{C,1}	14.7 (0.6) ^{D,2}	13.2 (0.6) ^{D,1}	13.3 (0.4) ^{E,1,2}	14.1 (1.0) ^{D,2}	12.8 (0.3) ^{C,1}
	TC		3.6 (0.5) ^{CD,1}	3.2 (0.6) ^{B,1,2}	3.4 (0.5) ^{B,1,2}	2.4 (0.9) ^{A,2}	3.6 (0.3) ^{B,C,1}	3.7 (0.1) ^{B,1}	1.8 (0.3) ^{A,2}

a,b,c,d,e Describe significant differences between orientations within one 3D printed material and ageing time ($p < 0.05$).

A,B,C,D,E Describe significant differences between materials within one ageing time ($p < 0.05$).

1,2,3,4 Describe significant differences between ageing times (compared to baseline) within one ageing media and one material ($p < 0.05$).

3.1.2. Resin materials

Statistical analysis using one-way ANOVA unveiled significant differences in both HM and E_{IT} among materials produced through milling and 3D printing methods, as well as within the different categories of materials: definitive (LU, CT, VCP) and temporary (TC, ND, DT, GC), both before and after aging.

Trends in HM at baseline decreased with statistical significance ($p < 0.05$) in the order of LU > CT > VCP > ND ≥ TC > DT ≥ GC. Nevertheless, after 90 days of ageing, the Martens parameters were found to be influenced by the interaction between the material group and storage time in both ageing media resulting in statistically

significant differences between materials ($p < 0.05$). LU specimens consistently displayed significantly higher HM and E_{IT} values compared to all other tested resin materials, both before and after aging in both media. The definitive 3D-printed materials, CT and VCP, exhibited statistically higher hardness than the temporary materials (TC, ND, DT, and GC) under dry conditions ($p < 0.05$). However, at the end of the aging period, TC and ND demonstrated similar HM and E_{IT} values to the definitive 3D-printed materials (CT and VCP) in AS. Nonetheless, in DW, TC still exhibited higher HM than the 3D-printed materials, while GC and DT consistently showed the lowest Martens parameters in both aging media.

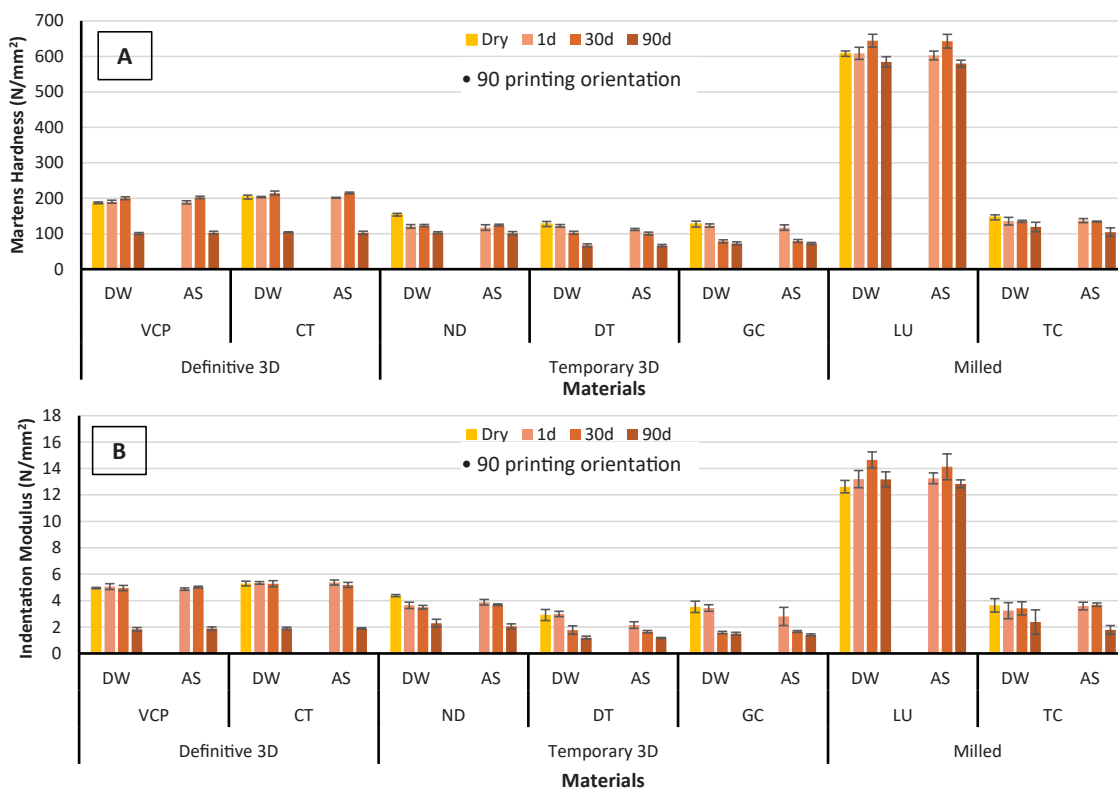


Fig. 3. (a) Martens hardness and (b) indentation modulus of 3D-printed (90° orientation) and milled resin materials before and after ageing in DW and AS for 90 days.

3.1.3. Ageing time and ageing media

No significant differences in both HM and E_{IT} were detected after 1 day of aging in either DW or AS for CT, GC, LU and TC. HM of ND and DT significantly decreased after 1 day compared to dry conditions, while VCP exhibited a significant increase in hardness compared to the baseline after 1 and 30 days of aging in both media. Furthermore, after 30 days of aging, LU, CT, and ND displayed increased HM compared to the measurements on day 1. Conversely, DT, GC, and TC exhibited lower HM at 30 days compared to day 1. Subsequently, there was a decline in both HM and E_{IT} across all studied materials after 90 days of aging in both DW and AS. The percentage change in hardness from the baseline (HR%) varied from 3.62% to 48.79% in DW and 4.39% to 49.5% in AS, as detailed in Table 5 and Fig. 4. Importantly, no statistically significant difference in hardness reduction between the two-aging media (DW and AS) was noted for all tested material except TC, where hardness reduction in DW was less than in AS.

Table 5

Mean and standard deviation values for hardness reduction percentage (HR%) of all studied materials after 90 days of storage in distilled water and artificial saliva.

Category	Material	Distilled water HR%	Artificial Saliva HR%	
3D-printed (90°)	Definitive VCP	46.3 (1.8) ^{A1}	45.0 (1.5) ^{A1}	
	CT	48.8 (1.0) ^{A1}	49.5 (3.1) ^{A1}	
	Temporary	ND	32.9 (3.0) ^{B1}	34.1 (3.1) ^{B1}
		DT	47.3 (4.3) ^{A1}	47.6 (1.7) ^{A1}
		GC	42.5 (3.7) ^{A1}	42.6 (5.9) ^{A1}
Milled	LU	3.6 (1.7) ^{C1}	4.4 (2.0) ^{C1}	
	TC	18.2 (11.3) ^{D1}	29.2 (6.8) ^{B2}	

Values with the same superscript letters in a column represent a non-significant difference between materials ($p > 0.05$). Values with the same superscript numbers in a row indicate a non-significant difference between ageing media ($p > 0.05$).

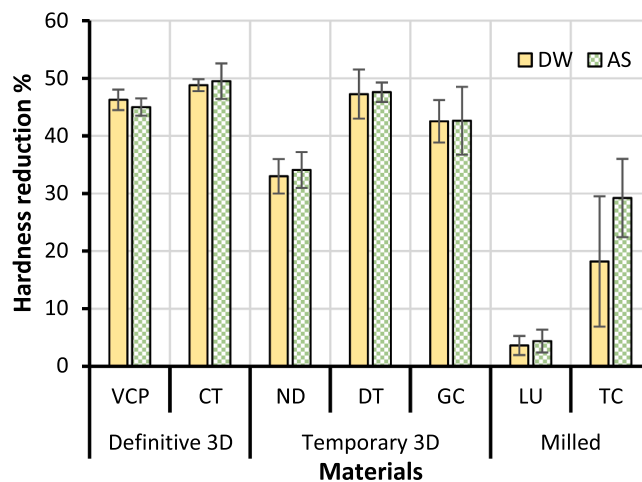


Fig. 4. Hardness reduction percentage (HR%) of 3D-printed (90° orientation) and milled resin after 90 days of storage compared to baseline in DW and AS. Standard deviation is indicated through error bars.

3.2. Filler content (wt%)

Table 6 presents the average filler weight percentage for all the examined materials, determined through the ash technique (ISO 1172, 1996), and this data is compared to the manufacturer-provided information. The filler weight percentage exhibited statistically significant differences in the following order: LU > CT ≥ VCP > GC > ND > DT ($p < 0.05$). Notably, the filler weight percentages of VCP and CT were similar ($p = 0.9$). The filler weight of TC could not be measured as it is a PMMA material that does not contain any fillers.

Table 6
Mean and standard deviation values for filler content (wt%) of all studied materials measured using the ash method (n = 3).

Category		Material	Manufacturer filler wt%	Measured filler wt%
3D-Printed	Definitive	VCP	30-50	33.8 (0.3) ^b
		CT	30-50	33.4 (1.9) ^b
	Temporary	ND	Not disclosed	7.4 (0.1) ^d
		DT	Not disclosed	0.95 (0.1) ^e
		GC	10-25	19.5 (0.1) ^c
Milled	LU	80	73.5 (1.3) ^a	
	TC	N/A	N/A	

Values with the same superscript letters represent a non-significant difference between materials (p > 0.05).

3.3. Morphology of the superficial surface

A layering structure was evident in specimens printed with varying orientations, as shown in Fig. 5. Nonetheless, upon polishing to a depth

of approximately 0.3 mm into the sample, the layering structure disappeared. This suggests that the layering structure was confined to the superficial surface and was not present within the main body of the specimens.

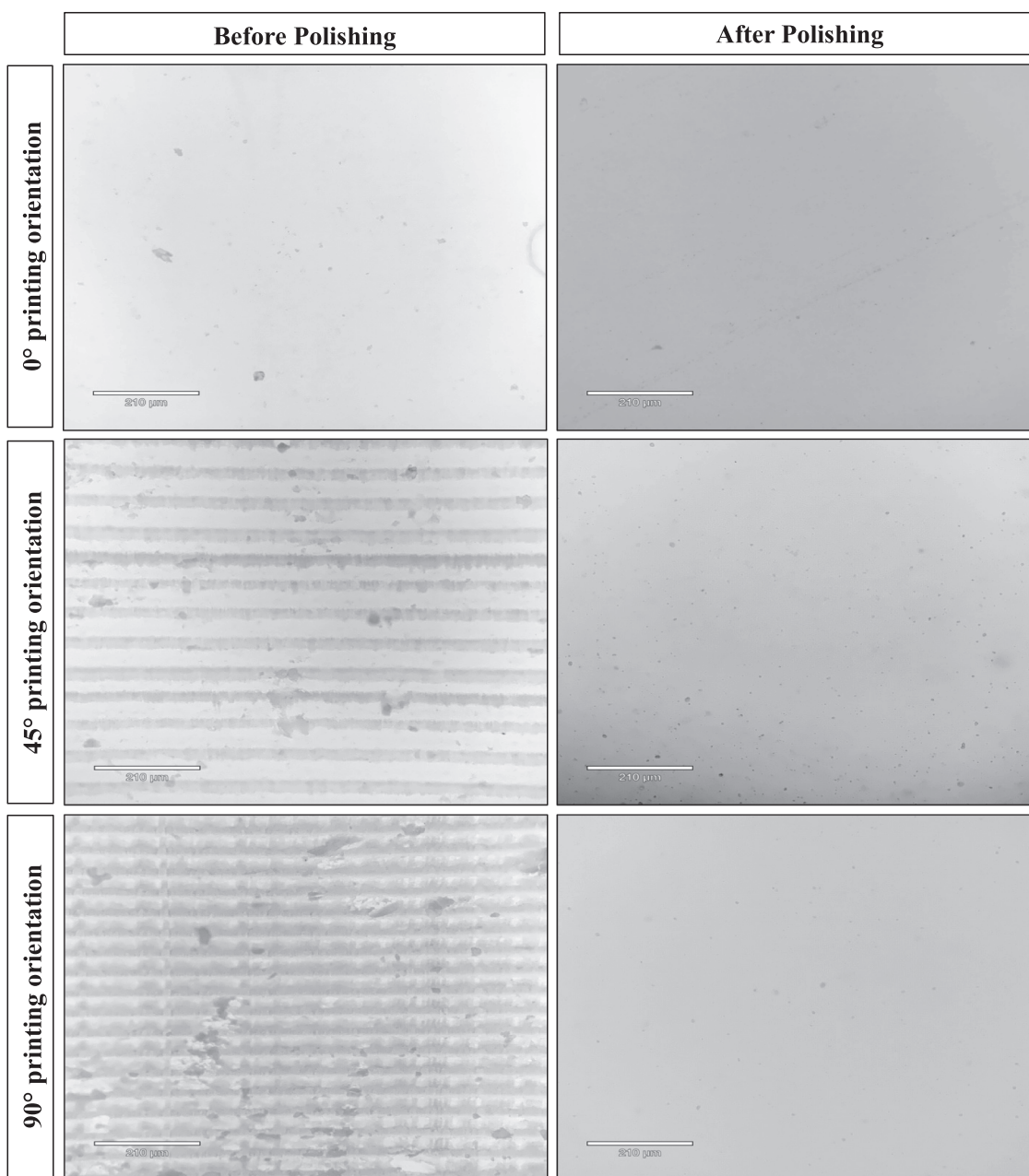


Fig. 5. Optical microscope images of 3D-printed resin material VCP showing the surface morphology with different layer orientations (Magnification 10 ×, Scale bar=210 µm). Images represent all 3D-printed resin materials.

4. Discussion

4.1. Summary of the study and hypothesis testing

In the present study, printing orientation had a non-significant impact on HM and E_{IT} values at baseline, as well as at the end of the ageing process, except for HM of VCP and ND specimens. Thus, the first null hypothesis was partially rejected. Meanwhile, significant differences in HM and E_{IT} were identified between the investigated materials before and after ageing, and the storage times had a significant impact on HM and E_{IT} . Therefore, the second and third null hypotheses were rejected. The results also indicated that there were no differences in HM and E_{IT} observed for each tested material between the two-aging media (DW and AS) throughout the entire study period, thus the fourth null hypothesis was accepted.

4.2. Printing orientation

In order to evaluate the resistance against stress of a restoration, like that from contact with an opposing surface, and indirectly assess chemical degradation, the changes in hardness of material specimens immersed in solvents were analysed [31]. Hardness serves as a measurable metric for the ability of a solid material to withstand compressive forces on its surface [32,33]. The Marten's test is a good approach to measuring the elastic-plastic behaviour of materials [34]. Traditionally, Vickers hardness utilising a light microscope was used to measure the permanent deformation area after removing the load. However, this method is influenced by operator subjectivity during optical readings and is less accurate for materials exhibiting elastic-plastic behaviour [32,34,35]. The HM test was developed to overcome these limitations, recording various quantitative parameters from the force-displacement curve, such as E_{IT} and creep [26,36]. Several parameters, including loading force, holding time, and ambient temperature, can affect HM values and need standardization [26]. This study followed the test parameters established by Fischer et al. [37] as they are suitable for polymer-based materials.

Slight yet statistically significant differences in HM and E_{IT} were noted between orientations for all 3D printed materials, except CT, under dry conditions and up to 30 days of ageing which could be explained by the anisotropic nature of 3D printed parts. Anisotropy implies that the force applied on the object can lead to varying impacts depending on whether it acts perpendicular or parallel to the layers [14, 38,39]. Similarly, a study by Alaqeel et al. [40] detected differences in nanohardness between occlusal splint materials printed at 0° and 90° orientations after 14 days of water storage. The 0° orientation exhibited less hardness which was linked to the presence of micropores observed in SEM images. However, it is crucial to consider that their study employed a layer thickness of 150 µm while this study employed a 50 µm thickness. On the other hand, a study by de Castro et al. [6] examined the impact of 0°, 45°, and 90° printing orientations on the mechanical properties of commercial 3D-printed PMMA provisional resins. Their study utilized Knoop hardness and a fixed layer thickness of 50 µm and found that build orientation did not affect the microhardness of the non-aged PMMA provisional resins. Furthermore, since an instrumented indentation method was employed, submicron surface irregularities, following polishing, can form indentations simply through touching of the filler or matrix. This produces values that do not accurately represent the homogenous material [41–43], which may also explain the differences in HM and E_{IT} of the investigated materials.

After subjecting 3D printed materials to 90 days of ageing in both DW and AS, it was evident that printing orientation did not significantly affect the Martens parameters across all materials. This could be attributed to the homogeneity of 3D printed specimens. As mentioned earlier, the layer thickness in this study was set at 50 µm, a choice supported by previous research showing no signs of sample delamination at layer boundaries when orientations between 0° and 45° were

employed, confirming the homogeneity of 3D-printed objects with similar layer thickness [44]. Furthermore, DLP printers polymerize each layer on the bottom of the printer vat, ensuring polymerization occurs without oxygen. Consequently, oxygen inhibition layers do not interfere with the adhesion between layers [30].

Each surface was meticulously polished following ISO 14577–4 (2016) standards [33], successfully establishing a smooth, irregularity-free surface before indentation testing and to remove the soft and weak resin-rich layers, as emphasized by Marghalani (2010). This polishing procedure effectively eliminated the visible printing layers on the 45° and 90° specimen surfaces (Fig. 5). Altarazi et al. [21], through SEM and optical microscope analysis, also confirmed that the 50 µm printing layers were visible only on the surface, not in the deeper layers, highlighting the overall homogeneity of the 3D printed materials.

4.3. Resin materials

Regarding materials, notable differences in Martens parameters were evident among 3D-printed and milled resin materials designated for both temporary and definitive restoration, both before and after undergoing aging processes. Several factors have been identified as contributors to these differences in surface hardness. These factors encompass the method of specimen production, the inherent material composition, the post-polymerization device used, and the artificial aging process [30].

In terms of production methods, resin composite blocks for subtractive manufacturing are created and polymerized under controlled temperatures and high pressure. This method enhances the degree of conversion (DC) and augments mechanical properties, leading to the production of a more consistent dental prostheses compared to conventional manufacturing techniques [45,46]. Conversely, restorations produced using a DLP 3D printer rely on light emitted from the printer to polymerize photosensitive materials layer by layer [47]; additional post-printing UV exposure is recommended by manufacturers to finalize the polymerization process, enhance the DC, and improve mechanical properties [48]. This distinction partly explains why materials created through subtractive methods exhibited higher hardness and elastic modulus compared to their 3D-printed counterparts, similar to other findings [18].

Regarding cleaning and post-polymerization devices for 3D printed parts, studies have suggested that the cleaning solution could impact various properties [17,49]. However, it is important to note that for all additive materials in this study, the cleaning solution and cleaning time were standardized. Furthermore, Reymus and Stawarczyk [30] emphasized the significant impact of post-polymerization devices on the Martens parameters of additively manufactured components. In this study, three specific post-polymerization devices were utilized based on the manufacturers' recommendations for each material, as detailed in Table 2. Specimens cured in the Otofash G171 (CT, VCP) and the Formcure unit (ND) had greater hardness compared to those cured in the Caraprint LED unit (DT). Unlike the other two photopolymerization devices, the Otofash unit does not deliver continuous irradiation; instead, it provides repeated concentrated flashes of light, potentially resulting in the specimens being exposed to a higher light intensity. Also, the OF unit covers the widest wavelength spectrum, stimulating a broader range of photoinitiators which positively influences the DC and, consequently, the hardness as proven by other studies [16,17,50]. On the other hand, the Formcure UV unit had the longest working time, lasting 30 min. This extended post-polymerization period may have positively impacted the polymerization of the ND specimens [51,52]. These factors help explain the higher hardness observed in definitive materials (VCP, CT) and ND compared to DT. It is noteworthy that this study adhered strictly to the post-curing recommendations of the manufacturers. However, standardizing the post-curing protocol could have led to different outcomes.

In terms of material composition, several factors play a crucial role in

influencing the mechanical properties of resin composites, including the composition of the inorganic phase, filler load, morphology, and distribution [53–55]. Among the tested materials, LU exhibited the highest filler load by weight (74%), followed by VCP and CT (33%), and GC (10–25%). In contrast, TC primarily consists of PMMA and lacks any fillers, while the filler load for ND and DT was not disclosed by their manufacturers but was measured to be 7.4% and 0.95%, respectively. The strong positive correlation between filler weight and HM explains why LU displayed higher Martens hardness than TC blocks and all 3D printed materials. This observation is in agreement with the findings of other studies on resin-based materials [56,57].

Additionally, LU contained silica particles with a diameter of 20 nm and zirconia particles ranging from 4–11 nm, further explaining the higher HM values compared to those of VCP and CT, which reported an average particle size of 0.7 μm (as per their manufacturer). Previous studies have indicated that composite materials incorporating smaller filler particles exhibit increased surface microhardness [58]. LU incorporates nanoclusters of non-aggregated, non-agglomerated silica and zirconia nanoparticles [59]. This specific filler shape, characterized by its non-spherical nature, has been found to result in higher elastic modulus and hardness values than materials containing spherical fillers, regardless of filler size [53,60]. Unfortunately, drawing conclusions about the 3D-printed materials studied in this research is challenging because information on their filler morphology is lacking.

Interestingly, despite containing fillers, GC exhibited lower HM compared to TC. This phenomenon could be attributed to the exfoliation and dislodgement of filler particles due to chemical degradation, indicating inadequate integration of the particles within the matrix [17]. It is important to note that adding fillers to 3D printable resins presents challenges, as suspended particles must not undergo sedimentation or agglomeration during the printing process [61]. Particle clustering increases inter-particle spacing, limiting the ability of the particles to protect the softer resin matrix from degradation [17,62], thereby influencing the mechanical coherence of the material and explaining the observed differences among the studied materials.

The hardness stability of 3D-printed materials after aging was significantly lower compared to milled materials. Hardness is influenced not only by filler loading but also by the resin-matrix composition and interactions occurring in the monomer mixture, as well as the resulting polymer network features [63]. LU has a matrix composition of UDMA and Bis-EMA, which contributes to a densely crosslinked network, enhancing durability and reducing polymerization shrinkage and material softening [64,65]. Unlike milled resin-composites, 3D-printed materials have strict viscosity requirements for optimal printing [66–68]. BisEMA, found only in CT, reduces viscosity, making it suitable for 3D printing, and also lowers water sorption due to its hydrophobic nature [69,70], explaining its higher hardness compared to temporary 3D-printed materials. GC, despite containing UDMA, exhibited low hardness, aligning with other findings [71], possibly due to its lower filler load and the presence of EDMA, which provides flexibility impacting overall hardness. However, this contradicts with the findings by Mayer et al. [17], possibly due to different test parameters or post-curing methods. Additionally, monomers like HEMA in ND, absorb water due to their hydrophilic nature, leading to swelling and reduced mechanical properties, potentially affecting hardness over time. However, ND showed comparable hardness to the definitive 3D-printable resins (CT and VCP) and milled PMMA resin (TC). Notably, ND displayed the lowest hardness reduction percentage among the 3D printed resins, which could be attributed to the post polymerisation device employed.

Considering these findings, the recently developed additive resins, specifically labelled as suitable for definitive restorations like VCP and CT, in addition to the temporary ND, appear to be more suitable for long-term use compared to those labelled as temporary (GC and DT), even though specific service duration is not specified by the manufacturers. This difference might be attributed to the polymerization strategy and

filler content and morphology. Additionally, encompassing a wider variety of materials would facilitate a more effective understanding of the increasingly available 3D-printable resins in the market.

4.4. Artificial ageing

Restorative dental materials are constantly exposed to diverse and aggressive environmental conditions during their clinical use, including biological, chemical, physical, and mechanical factors [36]. Storage in a wet medium, thermocycling, and fatigue testing are some of several valid methods for in vitro simulation of the ageing of FDPs in the oral cavity [72]. In this study, chemical degradation was simulated using DW and AS as storage media since they mimic the wet intra-oral environment [56,73] and effect mechanical properties of resin based materials [74–76]. The current study confirms previous research findings that DW and AS have similar effects in reducing hardness of resin-materials [77–80]. An exception was observed in the case of TC, where AS caused a more significant reduction in hardness compared to DW. Generally, the reduction in hardness was higher in AS than in DW. This difference could be attributed to the slightly acidic nature of AS, with a measured pH of 5.3. Since TC was the sole PMMA material and the only one without fillers, it might have been more susceptible to water sorption within its polymer network resulting in resin plasticizing and softening effects [81–84].

Previous research has indicated that significant changes in the hardness of resin-composites typically occur within a few days of exposure to solvents. However, the findings from this study suggest that significant results might not be observed after just one day of ageing. Furthermore, Bürgin et al. [85] suggested that 16 days of storage might not suffice for resin-composite materials proposing that 30 days should be the minimum duration, a perspective supported by several studies [56,78,86]. Considering the clinical relevance of long-term wet storage, this study was conducted over 90 days, a period during which most materials reach equilibrium [28,77,87–89].

In general, Martens parameters decreased after 1 day of wet storage compared to dry conditions (except for VCP and LU) due to initial water absorption and degradation of the resin matrix, as observed in earlier research [30]. However, the intriguing increase in HM values observed in some tested materials (VCP, CT, LU) after 30 days compared to 1 day of wet storage is noteworthy. This phenomenon has previously been found when testing direct resin-composite materials [76] and 3D-printed resin-composite materials used for temporary restorations [30]. A possible explanation for the observed rise in hardness likely stems from increased monomer conversion induced by a warm storage medium and/or supplementary cross-linking reactions occurring within the resin phase over time [90].

The current study has also highlighted the significant impact of prolonged ageing on the materials' Martens parameters. Generally, a decrease in HM was recorded with prolonged storage time. This outcome aligns with studies on resin-based materials and can be explained by water absorption [16,30,34,91] and the possibility of monomer elution in small quantities for up to twelve months [77,92–94].

Simulated aging using DW and AS only represented the chemical aspects of aging. Including simulated mastication, examining material stability under fluctuating temperature conditions, and investigating the effects of various solvents found in the oral cavity could have produced different outcomes.

4.5. Clinical significance

Considering HM and E_{IT} as crucial factors for assessing mechanical properties, 3D-printed resin-composites used in this study are promising. However, they do not seem to be at the level of milled materials that could affect their long term clinical performance.

5. Conclusions

Within the limitations of this study, the following can be concluded:

1. The impact of printing orientation on the Martens parameters of 3D-printed resin-composites was generally low, and the effect on HM varied depending on the material.
2. Both HM and E_{IT} were significantly influenced by the material group and storage time.
3. 3D-printed resins recommended for definitive restorations displayed higher Martens parameters compared to those intended for temporary use, with the exception of ND.
4. Milled resin-composite LU exhibited considerably higher HM and E_{IT} than 3D-printed materials at all-time intervals, while PMMA-based milled material TC showed similar values to the latter.
5. 3D-printed materials were more significantly impacted by ageing compared to the milled blocks.
6. Distilled water and artificial saliva had comparable effects on the hardness reduction of all investigated materials except TC.
7. Conclusions about the behaviour of resin materials cannot be drawn after just one day of wet storage; longer ageing periods are necessary for comprehensive analysis.

Disclosure

Given his role as Editor, Dr Nick Silikas had no involvement in the peer review of this article and has no access to information regarding its peer review. Full responsibility for the editorial process for this article was delegated to the Editor in Chief, Dr. David Watts.

Declaration of Competing Interest

The authors declare that they have no conflicts of interest related to the publication of this research.

Acknowledgements

The first author (Shaymaa Mudhaffer) was funded by a full-time scholarship by the Saudi Arabain Cultural Bureau in London, UK.

References

- [1] Della Bona A, Cantelli V, Britto VT, Collares KF, Stansbury JW. 3D printing restorative materials using a stereolithographic technique: a systematic review. *Dent Mater* 2021.
- [2] Espinar C, Della Bona A, Tejada-Casado M, Pulgar R, Pérez MM. Optical behavior of 3D-printed dental restorative resins: Influence of thickness and printing angle. *Dent Mater* 2023.
- [3] Jain S, Sayed ME, Shetty M, Alqahtani SM, Al Wadei MHD, Gupta SG, et al. Physical and mechanical properties of 3d-printed provisional crowns and fixed dental prosthesis resins compared to cad/cam milled and conventional provisional resins: A systematic review and meta-analysis. *Polymers* 2022;14:2691.
- [4] Stansbury JW, Idacavage MJ. 3D printing with polymers: Challenges among expanding options and opportunities. *Dent Mater* 2016;32:54–64.
- [5] Shim JS, Kim J-E, Jeong SH, Choi YJ, Ryu JJ. Printing accuracy, mechanical properties, surface characteristics, and microbial adhesion of 3D-printed resins with various printing orientations. *J Prosthet Dent* 2020;124:468–75.
- [6] de Castro EF, Nima G, Rueggeberg FA, Giannini M. Effect of build orientation in accuracy, flexural modulus, flexural strength, and microhardness of 3D-Printed resins for provisional restorations. *J Mech Behav Biomed Mater* 2022;136:105479.
- [7] Väyrynen VO, Tanner J, Vallittu PK. The anisotropy of the flexural properties of an occlusal device material processed by stereolithography. *J Prosthet Dent* 2016; 116:811–7.
- [8] Kessler A, Hickel R, Ilie N. In vitro investigation of the influence of printing direction on the flexural strength, flexural modulus and fractographic analysis of 3D-printed temporary materials. *Dent Mater J* 2021;40:641–9.
- [9] Unkovskiy A, Bui PH-B, Schille C, Geis-Gerstorf J, Huettig F, Spintzyk S. Objects build orientation, positioning, and curing influence dimensional accuracy and flexural properties of stereolithographically printed resin. *Dent Mater* 2018;34: e324–33.
- [10] Alshamrani AA, Raju R, Ellakwa A. Effect of printing layer thickness and postprinting conditions on the flexural strength and hardness of a 3D-printed resin. *BioMed Res Int* 2022;2022.
- [11] Alhazzawi TF. Advancements in CAD/CAM technology: Options for practical implementation. *J Prosthodont Res* 2016;60:72–84.
- [12] Alharbi N, Osman RB, Wismeijer D. Factors Influencing the Dimensional Accuracy of 3D-Printed Full-Coverage Dental Restorations Using Stereolithography Technology. *Int J Prosthodont* 2016;29:503–10.
- [13] Piedra-Cascón W, Krishnamurthy VR, Att W, Revilla-León M. 3D printing parameters, supporting structures, slicing, and post-processing procedures of vat-polymerization additive manufacturing technologies: A narrative review. *J Dent* 2021;109:103630.
- [14] Alharbi N, Osman R, Wismeijer D. Effects of build direction on the mechanical properties of 3D-printed complete coverage interim dental restorations. *J Prosthet Dent* 2016;115:760–7.
- [15] Silva NR, Moreira FGdG, Cabral AbdC, Bottino MA, Marinho RMDM, Souza RO. Influence of the postpolymerization type and time on the flexural strength and dimensional stability of 3D-printed interim resins. *J Prosthet Dent* 2023.
- [16] Reymus M, Stawarczyk B. Influence of different postpolymerization strategies and artificial aging on hardness of 3D-printed resin materials: an in vitro study. *Int J Prosthodont* 2020;33:634–40.
- [17] Mayer J, Reymus M, Mayinger F, Edelhoff D, Hickel R, Stawarczyk B. Temporary 3D-Printed Fixed Dental Prosthesis Materials: Impact of Postprinting Cleaning Methods on Degree of Conversion and Surface and Mechanical Properties. *Int J Prosthodont* 2021;34.
- [18] Berli C, Thieringer FM, Sharma N, Müller JA, Dedem P, Fischer J, et al. Comparing the mechanical properties of pressed, milled, and 3D-printed resins for occlusal devices. *J Prosthet Dent* 2020;124:780–6.
- [19] Huettig F, Kustermann A, Kuscü E, Geis-Gerstorf J, Spintzyk S. Polishability and wear resistance of splint material for oral appliances produced with conventional, subtractive, and additive manufacturing. *J Mech Behav Biomed Mater* 2017;75: 175–9.
- [20] Prpic V, Slacanin I, Schauerperl Z, Catic A, Dulcic N, Cimic S. A study of the flexural strength and surface hardness of different materials and technologies for occlusal device fabrication. *J Prosthet Dent* 2019;121:955–9.
- [21] Altarazi A, Haider J, Alhotan A, Silikas N, Devlin H. Assessing the physical and mechanical properties of 3D printed acrylic material for denture base application. *Dent Mater* 2022;38:1841–54.
- [22] Greil V, Mayinger F, Reymus M, Stawarczyk B. Water sorption, water solubility, degree of conversion, elastic indentation modulus, edge chipping resistance and flexural strength of 3D-printed denture base resins. *J Mech Behav Biomed Mater* 2023;137:105565.
- [23] Lee W-J, Jo Y-H, Yilmaz B, Yoon H-I. Effect of layer thickness, build angle, and viscosity on the mechanical properties and manufacturing trueness of denture base resin for digital light processing. *J Dent* 2023;104598.
- [24] Fusayama T, Katayori T, Nomoto S. Corrosion of gold and amalgam placed in contact with each other. *J Dent Res* 1963;42:1183–97.
- [25] El Mallakh B, Sarkar N. Fluoride release from glass-ionomer cements in de-ionized water and artificial saliva. *Dent Mater* 1990;6:118–22.
- [26] Czichos H, Saito T, Smith LE. Springer Handbook of Metrology and Testing. Springer Science & Business Media; 2011.
- [27] Greaves GN, Greer AL, Lakes RS, Rouxel T. Poisson's ratio and modern materials. *Nat Mater* 2011;10:823–37.
- [28] Alamoush RA, Sung R, Satterthwaite JD, Silikas N. The effect of different storage media on the monomer elution and hardness of CAD/CAM composite blocks. *Dent Mater* 2021;37:1202–13.
- [29] Alharbi N.A.B. Physico Mechanical Characterisation of a Novel and Commercial Cad/Cam Composite Blocks: The University of Manchester (United Kingdom); 2020.
- [30] Reymus M, Stawarczyk B. In vitro study on the influence of postpolymerization and aging on the Martens parameters of 3D-printed occlusal devices. *J Prosthet Dent* 2021;125:817–23.
- [31] Reymus M, Fabritius R, Keßler A, Hickel R, Edelhoff D, Stawarczyk B. Fracture load of 3D-printed fixed dental prostheses compared with milled and conventionally fabricated ones: The impact of resin material, build direction, post-curing, and artificial aging—An in vitro study. *Clin Oral Investig* 2020;24:701–10.
- [32] Broitman E. Indentation hardness measurements at macro-, micro-, and nanoscale: a critical overview. *Tribology Lett* 2017;65:23.
- [33] Ferracane J, Hilton T, Stansbury J, Watts D, Silikas N, Ilie N, et al. Academy of Dental Materials guidance—Resin composites: Part II—Technique sensitivity (handling, polymerization, dimensional changes). *Dent Mater* 2017;33:1171–91.
- [34] Shahdad SA, McCabe JF, Bull S, Rusby S, Wassell RW. Hardness measured with traditional Vickers and Martens hardness methods. *Dent Mater* 2007;23:1079–85.
- [35] Ashtiani AH, Azizian M, Rohani A. Comparison the degree of enamel wear behavior opposed to Polymer-infiltrated ceramic and feldspathic porcelain. *Dent Res J* 2019;16:71.
- [36] Babaier R, Watts DC, Silikas N. Effects of three food-simulating liquids on the roughness and hardness of CAD/CAM polymer composites. *Dent Mater* 2022;38: 874–85.
- [37] Fischer J, Roeske S, Stawarczyk B, Haemmerle CH. Investigations in the correlation between Martens hardness and flexural strength of composite resin restorative materials. *Dent Mater J* 2010;29:188–92.
- [38] Puebla K, Arcaute K, Quintana R, Wicker RB. Effects of environmental conditions, aging, and build orientations on the mechanical properties of ASTM type I specimens manufactured via stereolithography. *Rapid Prototyp J* 2012.
- [39] Nold J, Wesemann C, Rieg L, Binder L, Witkowski S, Spies BC, et al. Does printing orientation matter? In-vitro fracture strength of temporary fixed dental prostheses after a 1-year simulation in the artificial mouth. *Materials* 2021;14:259.

- [40] Alaqeel SM, Ramakrishnaiah R, Basavaraju RM, Kotha SB, Durgesh BH, Vallittu PK. Effect of 3D printing direction and water storage on nano-mechanical properties of 3D printed and auto-polymerized polymer with special emphasis on printing layer interface. *Mater Express* 2019;9:351–7.
- [41] Drummond JL. Nanoindentation of dental composites. *J Biomed Mater Res Part B: Appl Biomater: J Soc Biomater, Jpn Soc Biomater, Aust Soc Biomater Korean Soc Biomater* 2006;78:27–34.
- [42] El-Safty S, Akhtar R, Silikas N, Watts D. Nanomechanical properties of dental resin-composites. *Dent Mater* 2012;28:1292–300.
- [43] Issa Y, Watts DC, Boyd D, Price RB. Effect of curing light emission spectrum on the nanohardness and elastic modulus of two bulk-fill resin composites. *Dent Mater* 2016;32:535–50.
- [44] Grzebieluch W, Kowalewski P, Grygier D, Rutkowska-Gorczyca M, Kozakiewicz M, Jurczynszyn K. Printable and machinable dental restorative composites for cad/cam application—Comparison of mechanical properties, fractographic, texture and fractal dimension analysis. *Materials* 2021;14:4919.
- [45] Nguyen JF, Migonney V, Ruse ND, Sadoun M. Resin composite blocks via high-pressure high-temperature polymerization. *Dent Mater* 2012;28:529–34.
- [46] Balkenhol M, Mautner MC, Ferger P, Wöstmann B. Mechanical properties of provisional crown and bridge materials: chemical-curing versus dual-curing systems. *J Dent* 2008;36:15–20.
- [47] Dos Santos G, Alto RM, Sampaio Filho H, Da Silva E, Fellows C. Light transmission on dental resin composites. *Dent Mater* 2008;24:571–6.
- [48] Vitale A, Cabral JT. Frontal conversion and uniformity in 3D printing by photopolymerisation. *Materials* 2016;9:760.
- [49] Lankes V, Reymus M, Liebermann A, Stawarczyk B. Bond strength between temporary 3D printable resin and conventional resin composite: Influence of cleaning methods and air-abrasion parameters. *Clin Oral Investig* 2023;27:31–43.
- [50] Reymus M, Lümekemann N, Stawarczyk B. 3D-printed material for temporary restorations: impact of print layer thickness and post-curing method on degree of conversion. *Int J Comput Dent* 2019;22.
- [51] Kim D, Shim J-S, Lee D, Shin S-H, Nam N-E, Park K-H, et al. Effects of post-curing time on the mechanical and color properties of three-dimensional printed crown and bridge materials. *Polymers* 2020;12:2762.
- [52] Aati S, Chauhan A, Shrestha B, Rajan SM, Aati H, Fawzy A. Development of 3D printed dental resin nanocomposite with graphene nanoplatelets enhanced mechanical properties and induced drug-free antimicrobial activity. *Dent Mater* 2022;38:1921–33.
- [53] Kim K-H, Ong JL, Okuno O. The effect of filler loading and morphology on the mechanical properties of contemporary composites. *J Prosthet Dent* 2002;87:642–9.
- [54] Leprince J, Palin W, Mullier T, Devaux J, Vreven J, Leloup G. Investigating filler morphology and mechanical properties of new low-shrinkage resin composite types. *J Oral Rehabil* 2010;37:364–76.
- [55] Schwartz J, Söderholm KJ. Effects of filler size, water, and alcohol on hardness and laboratory wear of dental composites. *Acta Odontol Scand* 2004;62:102–6.
- [56] Hampe R, Lümekemann N, Sener B, Stawarczyk B. The effect of artificial aging on Martens hardness and indentation modulus of different dental CAD/CAM restorative materials. *J Mech Behav Biomed Mater* 2018;86:191–8.
- [57] Rosentritt M, Hahnel S, Schneider-Feyrer S, Strasser T, Schmid A. Martens hardness of CAD/CAM Resin-Based composites. *Appl Sci* 2022;12:7698.
- [58] Oja J, Lassila L, Vallittu PK, Garoushi S. Effect of accelerated aging on some mechanical properties and wear of different commercial dental resin composites. *Materials* 2021;14:2769.
- [59] Yin R, Kim Y-K, Jang Y-S, Lee J-J, Lee M-H, Bae T-S. Comparative evaluation of the mechanical properties of CAD/CAM dental blocks. *Odontology* 2019;107:360–7.
- [60] Masouras K, Silikas N, Watts DC. Correlation of filler content and elastic properties of resin-composites. *Dent Mater* 2008;24:932–9.
- [61] Taormina G, Sciancalepore C, Messori M, Bondioli F. 3D printing processes for photocurable polymeric materials: technologies, materials, and future trends. *J Appl Biomater Funct Mater* 2018;16:151–60.
- [62] Lim B-S, Ferracane JL, Condon JR, Adey JD. Effect of filler fraction and filler surface treatment on wear of microfilled composites. *Dent Mater* 2002;18:1–11.
- [63] Barszczewska-Rybarek IM. Structure-property relationships in dimethacrylate networks based on Bis-GMA, UDMA and TEGDMA. *Dent Mater* 2009;25:1082–9.
- [64] Sideridou I, Tserki V, Papanastasiou G. Study of water sorption, solubility and modulus of elasticity of light-cured dimethacrylate-based dental resins. *Biomaterials* 2003;24:655–65.
- [65] Söderholm K-J, Zigan M, Ragan M, Fischlschweiger W, Bergman M. Hydrolytic degradation of dental composites. *J Dent Res* 1984;63:1248–54.
- [66] Ligon SC, Liska R, Stampfl Jr, Gurr M, Mulhaupt R. Polymers for 3D printing and customized additive manufacturing. *Chem Rev* 2017;117:10212–90.
- [67] Manapat JZ, Chen Q, Ye P, Advincula RC. 3D printing of polymer nanocomposites via stereolithography. *Macromol Mater Eng* 2017;302:1600553.
- [68] Weng Z, Zhou Y, Lin W, Senthil T, Wu L. Structure-property relationship of nano enhanced stereolithography resin for desktop SLA 3D printer. *Compos Part A: Appl Sci Manuf* 2016;88:234–42.
- [69] Putzeys E, De Nys S, Cokic SM, Duca RC, Vanoirbeek J, Godderis L, et al. Long-term elution of monomers from resin-based dental composites. *Dent Mater* 2019;35:477–85.
- [70] Gajewski VE, Pfeifer CS, Fróes-Salgado NR, Boaro LC, Braga RR. Monomers used in resin composites: degree of conversion, mechanical properties and water sorption/solubility. *Braz Dent J* 2012;23:508–14.
- [71] Husain NA-H, Feilzer AJ, Kleverlaan CJ, Abou-Ayash S, Özcan M. Effect of hydrothermal aging on the microhardness of high-and low-viscosity conventional and additively manufactured polymers. *J Prosthet Dent* 2022;128:822. e1–. e9.
- [72] Szczesio-Wlodarczyk A, Sokolowski J, Kleczewska J, Bociong K. Ageing of dental composites based on methacrylate resins—A critical review of the causes and method of assessment. *Polymers* 2020;12:882.
- [73] Correr GM, Bruschi Alonso RC, Baratto-Filho F, Correr-Sobrinho L, Sinhoretto MAC, Puppini-Rontani RM. In vitro long-term degradation of aesthetic restorative materials in food-simulating media. *Acta Odontol Scand* 2012;70:101–8.
- [74] Yap A, Tan S, Wee S, Lee C, Lim E, Zeng K. Chemical degradation of composite restoratives. *J Oral Rehabil* 2001;28:1015–21.
- [75] Yap A, Chung S, Rong Y, Tsai K. Effects of aging on mechanical properties of composite restoratives: A depth-sensing microindentation approach. *OPERATIVE Dent-Univ Wash* 2004;29:547–53.
- [76] Hahnel S, Henrich A, Bürgers R, Handel G, Rosentritt M. Investigation of mechanical properties of modern dental composites after artificial aging for one year. *Oper Dent* 2010;35:412–9.
- [77] Alshali RZ, Salim NA, Sung R, Satterthwaite JD, Silikas N. Analysis of long-term monomer elution from bulk-fill and conventional resin-composites using high performance liquid chromatography. *Dent Mater* 2015;31:1587–98.
- [78] Liebermann A, Wimmer T, Schmidlin PR, Scherer H, Löffler P, Roos M, et al. Physicochemical characterization of polyetheretherketone and current esthetic dental CAD/CAM polymers after aging in different storage media. *J Prosthet Dent* 2016;115:321–8. e2.
- [79] Sideridou ID, Karabela MM. Sorption of water, ethanol or ethanol/water solutions by light-cured dental dimethacrylate resins. *Dent Mater* 2011;27:1003–10.
- [80] Alamoudi RA, Salim NA, Silikas N, Satterthwaite JD. Long-term hydrolytic stability of CAD/CAM composite blocks. *Eur J Oral Sci* 2022;130:e12834.
- [81] Niem T, Youssef N, Wöstmann B. Influence of accelerated ageing on the physical properties of CAD/CAM restorative materials. *Clin Oral Investig* 2020;24:2415–25.
- [82] Ferracane J, Condon J. Degradation of composites caused by accelerated aging. *J Dent Res* 1991;70:480.
- [83] Ferracane JL. Hygroscopic and hydrolytic effects in dental polymer networks. *Dent Mater* 2006;22:211–22.
- [84] Ayşe Atay D, Elçin Sağırkaya D. Effects of different storage conditions on mechanical properties of CAD/CAM restorative materials. *Odovtos-Int J Dent Sci* 2020;22:83–96.
- [85] Bürgin S, Rohr N, Fischer J. Assessing degradation of composite resin cements during artificial aging by Martens hardness. *Head face Med* 2017;13:1–7.
- [86] Alrobeigy NA. Mechanical properties of contemporary resin composites determined by nanoindentation. *Tanta Dent J* 2017;14:129–38.
- [87] Van Landuyt K, Nawrot T, Geebelen B, De Munck J, Snauwaert J, Yoshihara K, et al. How much do resin-based dental materials release? A meta-analytical approach. *Dent Mater* 2011;27:723–47.
- [88] Łagocka R, Mazurek-Mochol M, Jakubowska K, Bendyk-Szeffer M, Chlubek D, Buczkowska-Radlińska J. Analysis of base monomer elution from 3 flowable bulk-fill composite resins using high performance liquid chromatography (HPLC). *Med Sci Monit: Int Med J Exp Clin Res* 2018;24:4679.
- [89] Al Sunbul H, Silikas N, Watts DC. Surface and bulk properties of dental resin-composites after solvent storage. *Dent Mater* 2016;32:987–97.
- [90] De Moraes RR, Marimon JLM, Jochims Schneider LF, Sinhoretto MAC, Correr-Sobrinho L, Bueno M. Effects of 6 months of aging in water on hardness and surface roughness of two microhybrid dental composites. *J Prosthodont* 2008;17:323–6.
- [91] Chicot D, Mercier D, Roudet F, Silva K, Staia M, Lesage J. Comparison of instrumented Knoop and Vickers hardness measurements on various soft materials and hard ceramics. *J Eur Ceram Soc* 2007;27:1905–11.
- [92] Polydorou O, Huberty C, Wolkewitz M, Bolek R, Hellwig E, Kümmerer K. The effect of storage medium on the elution of monomers from composite materials. *J Biomed Mater Res Part B: Appl Biomater* 2012;100:68–74.
- [93] Polydorou O, König A, Hellwig E, Kümmerer K. Long-term release of monomers from modern dental-composite materials. *Eur J Oral Sci* 2009;117:68–75.
- [94] Polydorou O, Trittler R, Hellwig E, Kümmerer K. Elution of monomers from two conventional dental composite materials. *Dent Mater* 2007;23:1535–41.